

Pulse Radiolysis of Nitrobenzene in Aqueous Solutions Containing Colloidal Platinum

Gad S. Nahor and Joseph Rabani*

Energy Research Center and The Department of Physical Chemistry, The Hebrew University of Jerusalem, Jerusalem 91904, Israel (Received: September 12, 1984; In Final Form: June 6, 1985)

The pulse radiolysis of nitrobenzene (NB) in aqueous solutions containing 2-propanol in the presence of colloidal Pt has been studied. The NB^- anion decays away by a single first-order process. The rate of decay is also first order in colloidal platinum (Ptc). The rate depends on the pH of the solutions. At relatively high pHs, hydrogen reduces NB and this reaction is mediated by the Ptc. Irreversible redox processes which produce nitrosobenzene and phenylhydroxylamine also take place, competing effectively with hydrogen formation.

Introduction

Nitrobenzene (NB) was found to be an efficient electron acceptor in photochemical redox systems where negatively charged photosensitizers such as tetrakis(sulphonatophenyl)porphyrin¹ and its Zn complex² are involved. NB has a standard redox potential $E^\circ(\text{NB}/\text{NB}^-) = -0.486$ V vs. NHE³ in water, and hence is capable of reducing water to H_2 . A system consisting of the NB^- anion radical is therefore of potential value in photochemical conversion and storage of solar light. In this contribution we report studies on the reactions of the NB^- radical ion in the presence of colloidal platinum using the pulse radiolysis technique. This system was chosen since under similar conditions methylviologen (MV^{2+}), which is a well-studied electron acceptor in photochemical systems⁴ and possesses a similar redox potential (-0.446 vs. NHE)⁵, has been found to react with Ptc⁶ and yield H_2 ⁶ by a hydride mechanism.^{6h}

Experimental Section

Materials. All reagents were of analytical grade. 2-Propanol (J. T. Baker) and acetone (J. T. Baker) were used as received. Nitrobenzene (BDH) was purified by vacuum distillation before use. Buffers consisted of 0.005 M standard buffer solutions⁷ containing CH_3COONa , CH_3COOH , KH_2PO_4 , Na_2HPO_4 , $\text{Na}_2\text{B}_4\text{O}_7$, HClO_4 , and NaOH . The preparation of the Pt colloids has been described previously.^{6h} The size of the colloid particles prepared by this method is 50 ± 5 Å;^{6h} thus the actual concentration of Ptc is about 4000 times smaller than the formal platinum concentration.^{6h} This was confirmed by kinetic measurements of the decay of methylviologen in the presence of Ptc. As previously reported^{6h} there are small quantitative variations in the results of different batches due to deviation in particle size. To

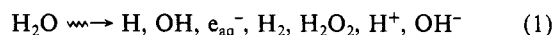
enable a comparison of results, batch identification numbers are stated whenever appropriate.

Unless otherwise stated, all solutions were deaerated by bubbling high-purity He (Matheson). The temperature was maintained at 21 ± 2 °C.

Apparatus. UV-visible spectra were recorded on a Bausch & Lomb Model Spectronics 2000 spectrophotometer. Pulse radiolysis experiments were carried out on a Varian 7715 linear accelerator with pulse duration varying from 0.5 to 1.5 μs with 200-mA current of 5 MeV. The total concentration of radicals ranged from 9.6×10^{-6} to 3.0×10^{-5} M. Dosimetry was measured using the initial absorption of NB^- at 313 nm ($\epsilon = 2930$ $\text{M}^{-1} \text{s}^{-1}$). Irradiation cells were of high-purity silica and were 0.5 or 1.0 cm long with one or three light passes. An Xe-Hg lamp was used as the analytical light source and the Hg lines at 303, 313, 335, and 365 nm were used as detection wavelengths. Appropriate filters were used to cut off light under 300 nm. A Hilger and Watts grating double monochromator with a IP28 photomultiplier was employed. The signal was transferred via a Biomation 3100 and an analog-to-digital convertor to a Nova 1200 minicomputer. H_2 measurements were carried out with a Varian aerograph Model 90P gas chromatography equipped with a Gow-Mack TC detector. High-purity Ar (3.6 L/min) was used as the gas carrier. The column, $1/8$ in. wide and 6 ft long, was filled with molecular sieve 5 Å. Solutions in which hydrogen measurements were taken were used in penniclyne type vials crimped with a rubber seal.

Results

When a solution containing 0.2 M 2-propanol and NB is pulse irradiated, processes 1-8 predominantly take place.⁸⁻¹¹ This



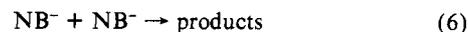
$$G = (0.6), (2.7), (2.7), (0.45), (0.75), (3.5), (0.8)$$



$$k_4 = 3.0 \times 10^{10} \text{ M}^{-1} \text{ s}^{-1} \text{ (ref 9)}$$



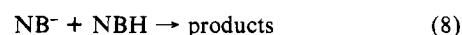
$$k_5 = (1.6-3.0) \times 10^9 \text{ M}^{-1} \text{ s}^{-1} \text{ (ref 11)}$$



$$k_6 = (1.0 \pm 0.1) \times 10^3 \text{ M}^{-1} \text{ s}^{-1} \text{ (ref 11, 12)}$$



$$K_7 = 1.6 \times 10^3 \text{ M}^{-1} \text{ (ref 11)}$$



$$k_8 = (1.7 \pm 0.9) \times 10^9 \text{ M}^{-1} \text{ s}^{-1} \text{ (ref 12)}$$

(1) G. S. Nahor, J. Rabani, and F. Griezer, *J. Phys. Chem.*, **85**, 697 (1981).

(2) G. S. Nahor and J. Rabani, *J. Phys. Chem.*, **89**, 2468 (1985).

(3) D. Meisel and P. Neta, *J. Am. Chem. Soc.*, **97**, 5198 (1975).

(4) See, for example, (a) C. R. Back, T. J. Meyer, and D. G. Whitten, *J. Am. Chem. Soc.* **96**, 4710 (1979); (b) A. Harriman, A. Porter and M.-C. Richoux, *J. Chem. Soc., Faraday Trans. 2*, **77**, 833 (1981); (c) I. Okura and N. Kim Thuan, *J. Chem. Soc., Chem. Commun.* **84** (1980); (d) I. Okura, S. Aono, M. Takeuchi, and S. Kusunoki, *Bull. Chem. Soc. Jpn.*, **55**, 3637 (1982); (e) J. Kiwi and M. Gratzel, *J. Am. Chem. Soc.*, **101**, 7214 (1979); (f) M. Rougee, T. Ebessen, F. Ghetti, and R. V. Bensasson, *J. Phys. Chem.*, **86**, 4404 (1982); (g) T. Ohsako, T. Sakamoto, and T. Matsuo, *Chem. Lett.*, 1675 (1983).

(5) M. W. Clark, "Oxidation Reduction Potentials of Organic Systems", Robert E. Krieger Publishing Company, Huntington, N. Y., 1972, and references cited therein.

(6) (a) A. Harriman, G. Porter, and M. C. Richoux, *J. Chem. Soc., Faraday Trans. 2*, **77**, 1939 (1981); (b) E. Sutcliffe and M. Neuman-Spallart, *Helv. Chim. Acta*, **64**, 2148 (1981); (c) O. Johansen, A. Launikonis, J. W. Loder, A. W. H. Mau, H. F. Sasse, J. D. Swift, and D. Wells, *Aust. J. Chem.*, **34**, 981 (1981); (d) P. Maillard, S. Caspard, P. Krausz, and C. Giannotti, *J. Organometal. Chem.*, **202**, 185 (1981); (e) D. S. Miller, A. J. Bard, G. McLendon, and J. Ferguson, *J. Am. Chem. Soc.*, **103**, 5336 (1981); (f) A. Demortier, M. De Backer, and G. Lepoutre, *Nouv. J. Chim.*, **7**, 421 (1983); (g) M. S. Matheson, P. C. Lee, D. Meisel, and E. Pelizzetti, *J. Phys. Chem.*, **87**, 394 (1983); (h) M. Brandeys, G. S. Nahor, and J. Rabani, *J. Phys. Chem.*, **88**, 1615 (1984); (i) M. Venturi, Q. G. Mulazzani, and M. Z. Hoffman, *J. Phys. Chem.*, **88**, 92 (1984). See also references cited therein.

(7) "Lange's Handbook of Chemistry", J. A. Deen, Ed., McGraw-Hill, New York, 1978, pp 5-77, 5-78.

(8) M. S. Matheson and L. M. Dorfman, "Pulse Radiolysis", The MIT Press, Cambridge, MA, 1969, and references cited therein.

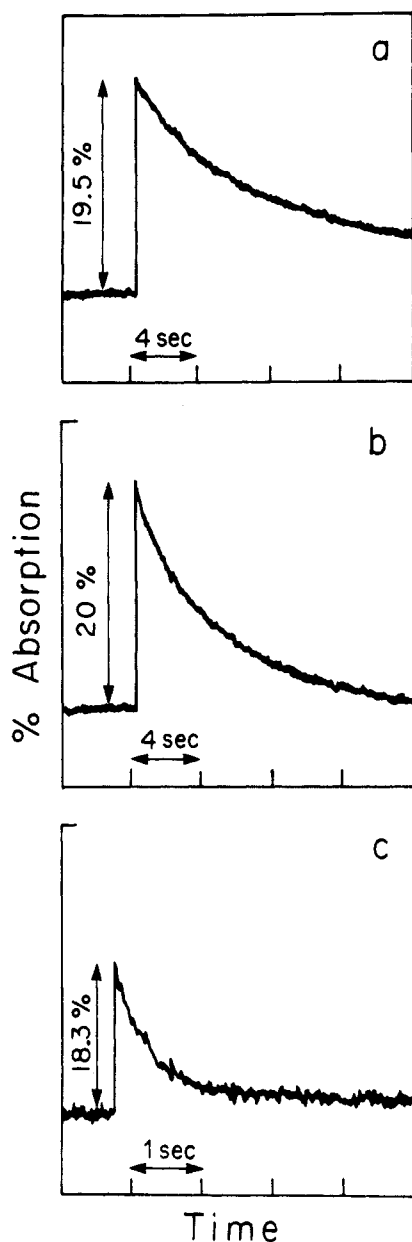


Figure 1. The decay of NB^- in the presence of and absence of Pt: (a) 4×10^{-4} M NB, 0.2 M 2-propanol, pH 8.0, 1-cm light pass; (b) 4×10^{-4} M NB, 0.2 M 2-propanol, 4×10^{-5} M [Pt], batch 2812, pH 8.0, 1-cm light pass; (c) same conditions as in b but with 4×10^{-4} M Pt.

reaction scheme predicts that the NB^- will decay away by a second-order, pH-dependent rate law with an apparent reaction rate constant $k_{\text{obsd}} = k_8 K_7 [\text{H}^+] + k_6$. Due to the pH dependence of the decay of NB^- most of this work was carried out at pH 8.0, where the decay rate is near its limiting value.^{10,12} Figure 1 shows that upon addition of colloidal Pt, the lifetime of NB^- is shortened and a nearly first-order rate law in NB^- is observed. The rate of decay of NB^- was found to be dependent on the Ptc concentration at well as on the pH, but not on the NB concentration. These effects will be discussed below. Some residual absorption remained after all the NB^- had decayed away. This is attributed to changes in light scattering by the colloidal particles as a result of small changes in their size. A similar result has been reported

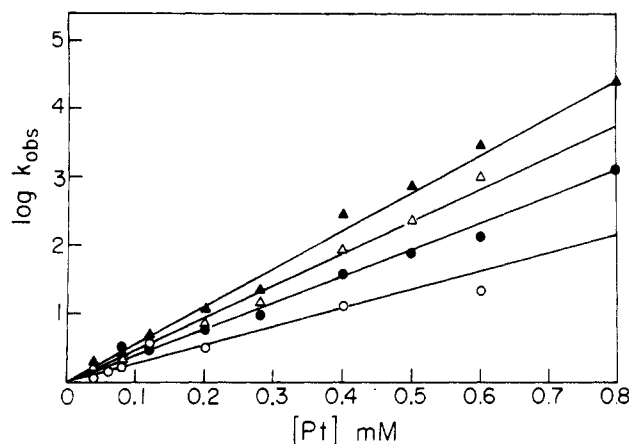


Figure 2. Effect of Pt concentration on the decay of NB^- : $\lambda_{\text{det}} = 313$ nm, 1.5- μs pulse, 1-cm light pass, 4×10^{-4} M NB, 0.2 M 2-propanol, pH 8.0. The first-order rate constant plotted against [Pt]. (\blacktriangle) 1.5- μs pulse, 313 nm, batch 2712; (\triangle) 0.5- μs pulse, 313 nm, batch 2712; (\bullet) 1.5- μs pulse, 365 nm, batch 2712; (\circ) 1.5- μs pulse, 313 nm, batch 2806.

for the Ptc-methylviologen system.^{6g,h}

Effect of Ptc Concentration

The Ptc concentration was varied in the range 4×10^{-5} to 8×10^{-4} M (formal Pt concentration). At relatively high [Pt], the decay of NB^- is strictly first order. At the lowest Ptc concentrations, deviations from first-order rate law are observed: the rate becomes slower as the reaction proceeds. The effect of [Pt] on the pseudo-first-order rate constant for NB^- decay (best fits up to 90% reaction) showed a linear dependence on [Pt], as can be seen in Figure 2. The results of experiments such as described in Figure 2 yield $k_9 = (4.7 \pm 1) \times 10^3$ (batch no. 2712) or $(2.7 \pm 0.8) \times 10^3 \text{ M}^{-1} \text{ s}^{-1}$ (batch no. 2806).



In view of the large effect of the size of the colloids on the actual Ptc concentration we consider these two values as being in agreement. It should be noted that since the radiation-induced radicals are produced homogeneously in the solution the effects observed here are due to NB^- which is produced in the bulk.

Effect of pH

The pH of the solution was varied in the range 6.1–13 keeping constant both [NB] and the formal [Pt] at 4×10^{-4} M, at ionic strength 0.05 M. Typical time profiles are shown in Figure 3. The results are summarized in Table I. In both acidic and slightly alkaline pHs, a single nearly first-order process is observed by which NB^- decays away. However, when the pH is above 11, an additional process involving a buildup of the absorbance is observed prior to the decay of the NB^- absorption (Figure 3c). In order to check the nature of the species responsible for this additional absorbance, we compared the absorbance 20 ms after the pulse (D_{∞}) to the absorbance at the maximal buildup (D_{Oid}). The results at four different wavelengths are presented in Table II. The ratio $D_{\text{Oid}}/D_{\infty}$ is unaffected by wavelength. Thus we conclude that the building up process produced additional NB^- . As will be discussed later, this process is attributed to an equilibration reaction of NB with Ptc which was preloaded by molecular hydrogen, similarly to the process observed at high pHs in the MV^{2+} -Ptc system.^{6h}

In Table I and Figure 4 we present the effect of pH on the rate of NB^- decay. The plot of the $\log k_9$ vs. pH yields a straight line with a slope of (-0.5 ± 0.1) , meaning a linear dependence of k_9 on $[\text{H}^+]^{1/2}$.

Varying NB Concentrations. The NB concentration was varied from 4×10^{-4} to 8×10^{-3} M at formal 4×10^{-4} M Ptc (batch 2006) at pH 8.0. The results of the highest and lowest concentrations used are shown in Figure 5. No [NB] effect was observed either on the initial absorption or on the decay rate of NB^- . This result is in contrast to our finding in the MV^{2+} /Ptc system^{6h} where MV^{2+} inhibited the decay of MV^+ .

(9) (a) E. J. Hart, S. Gordon, and J. K. Thomas, *J. Phys. Chem.*, **68**, 1271 (1964); (b) M. Anbar and E. J. Hart, *J. Am. Chem. Soc.*, **86**, 5633 (1964).

(10) J. Lilie, G. Beck, and A. Henglein, *Ber. Bunsenges. Phys. Chem.*, **75**, 458 (1971).

(11) K.-D. Asmus, A. Wigger, and A. Henglein, *Ber. Bunsenges. Phys. Chem.*, **70**, 862 (1966).

(12) G. S. Nahor and J. Rabani, *J. Phys. Chem.*, in press.

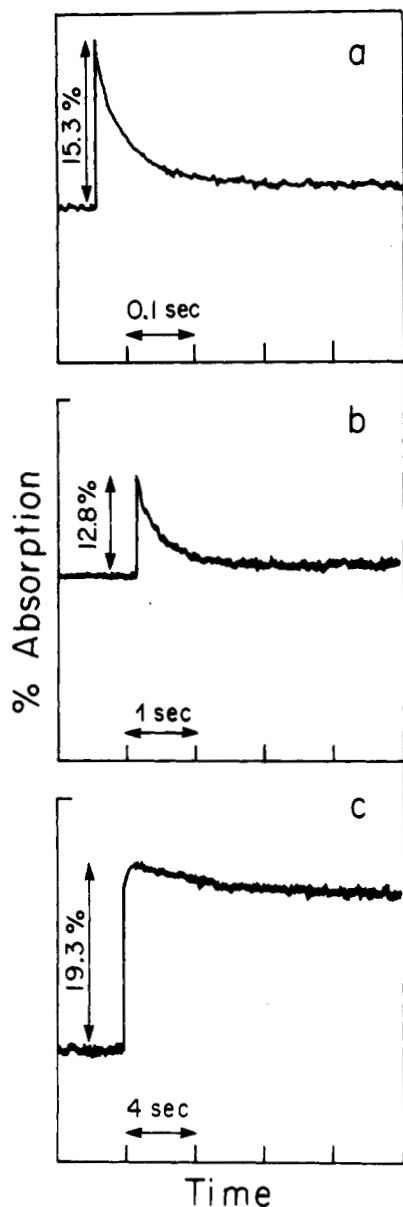


Figure 3. pH dependence of the decay of NB^- in the presence of Ptc: 4×10^{-4} M NB, 4×10^{-4} M [Pt], $1.5\text{-}\mu\text{s}$ pulse, $\lambda = 313$ nm. (a) pH 6.1, Pt batch 0105; (b) pH 9.0, Pt batch 0404; (c) pH 12, Pt batch 0404.

Bubbling H_2 . H_2 was bubbled through a solution containing 4×10^{-4} M NB at pH 12. Upon the addition of small concentrations of Ptc, and only then, a yellow color immediately appeared. The absorption spectrum of this yellow species is shown in Figure 6. It disappears within a few minutes. Removing the hydrogen by bubbling with He did not significantly affect the rate of the fading of this color. The color did not appear at $\text{pH} \leq 9$. After the color has faded, it reappears only upon addition of NB, but not upon addition of Ptc.

Semiquantitative Measurements of H_2 . Solutions containing 4×10^{-4} M NB and 0.2 M 2-propanol were given 30 pulses each of $1.5\text{-}\mu\text{s}$ duration, at a rate of 400 pulses/s. Hydrogen was measured and its relative concentration is reported in Table III. When Ptc was present, no hydrogen was observed either in the presence or in the absence of NB. In the absence of NB, acetone was added to the solution in order to scavenge the hydrated electrons. Acetone is reduced by e_{aq}^- to give the same radical species that are produced by reactions 2 and 3. In the absence of Ptc, the G for H_2 is expected to be 1.0.⁸ Indeed, a relatively large amount of H_2 was detected under such conditions, both in the presence and in the absence of NB.

Finally, when H_2 was injected into a solution containing Ptc only (buffered at pH 4), a significant part of the H_2 disappeared.

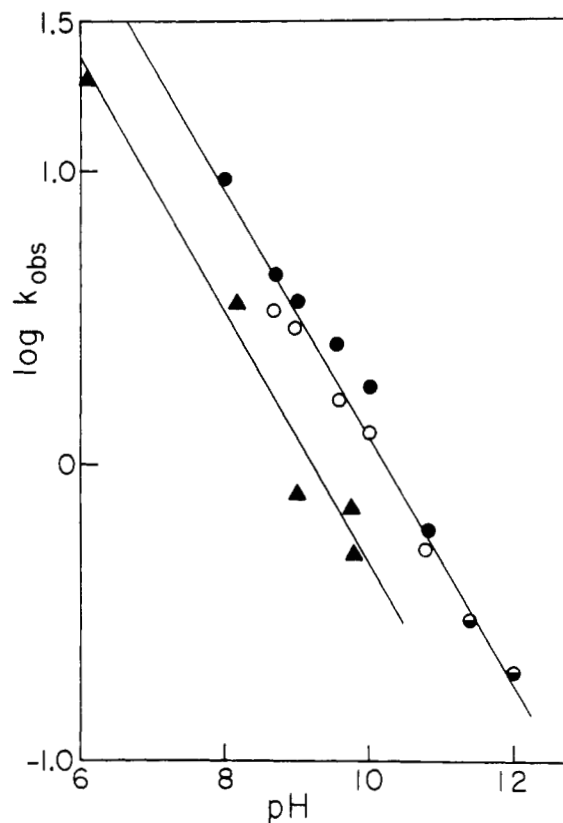


Figure 4. The effect of pH on the decay rate constant: (O, ●) Pt batches 0404 and 2006; (▲) Pt batches 0901 and 0105.

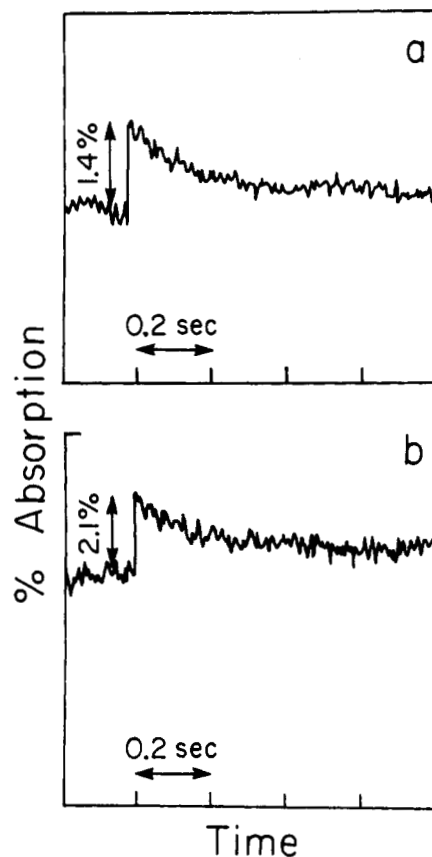


Figure 5. Effect of NB concentration: (a) 4×10^{-4} M NB, 4×10^{-4} M Pt, pH 8.0, $1.5\ \mu\text{s}$, 365 nm, 1-cm light pass; (b) 8×10^{-3} M NB.

These results will be discussed in the following.

Discussion

Comparison of the NB^- -Ptc and the MV^{2+} -Ptc systems⁶ shows

TABLE I: Effect of pH on the Decay of NB⁻ in the Presence of Ptcⁱ

pH	D_{∞}^e	D_{0d}^f	$D_{\infty d}^g$	k_{bu}^h	k_d^j		log k_d , 1.5
					1.5	0.5	
6.1 ^a	0.070	0.060	0.007		19	21	1.28
8.0 ^b	0.062	0.056	0.007		9.7	9.4	
8.2 ^c	0.092	0.093	0.010		3.4	3.7	0.53
8.7 ^d	0.064		0.010		3.4	4.5	0.53
9.0 ^d	0.070		0.005		2.9	3.6	0.46
9.0 ^c	0.096	0.088	0.010		0.8	0.8	-0.10
9.6 ^d	0.071		0.011		1.7	2.6	+0.23
9.8 ^c	0.099	0.072	0.012		0.5	0.7	-0.30
10.0 ^d	0.068				1.3	1.8	0.11
10.75 ^d	0.057		0.015		0.5	0.6	-0.30
11.0 ^d	0.070		0.009		1.8	2.1	0.26
11.4 ^d	0.077	0.090	≤0.010			0.3	-0.52
11.4 ^c	0.095	0.101		3.1/4.2			
12.0 ^d	0.082			4.7		0.2	-0.70
13.0 ^a	0.059	0.070		2.9 ± 0.3			

^aBatch 0105. ^bBatch 2006. ^cBatch 0901. ^dBatch 0404. ^eOptical densities (D) measured at the end of reaction 5. ^fOptical density at the beginning of the decay process taken on a slow time scale. $D_{0d} > D_{\infty}$ at the relatively high pHs due to conversion of molecular H₂ to NB⁻. At low pHs, D_{0d} is sometimes smaller than D_{∞} ; we attribute this to small traces of O₂. ^gResidual absorption after the decay occurred. ^hFirst-order rate constant of buildup process (whenever observed). ⁱ[NB] = 4 × 10⁻⁴ M, [Ptc] = 4 × 10⁻⁴ M (formal); λ_{det} = 313 nm, pulse duration 0.5 and 1.5 μs; 1.0-cm light pass. ^jRate constant (first order) of decay at two pulse intensities (1.5- and 0.5-μs pulse durations).

TABLE II: Comparison between Absorbances at the End of Process 5 (D_{∞}) and at Maximum Buildup (D_{0d})^a

λ, nm	D_{∞}	D_{0d}	D_{0d}/D_{∞}
303	0.101 ± 2%	0.109 ± 3%	1.08 ± 5%
313	0.061 ± 7%	0.070 ± 3%	1.15 ± 10%
335	0.009 ± 15%	0.012 ± 10%	1.33 ± 25%
365	0.007 ± 20%	0.008 ± 20%	1.14 ± 40%

^a[NB] = 4 × 10⁻⁴ M, [Pt] = 4 × 10⁻⁴ M (formal concentration) batch 0105; pH 13, 1.5-μs pulse, 3-cm light pass.

TABLE III: Results of Gas Chromatography Measurement for H₂

expt	2PrOH ^a	Acetone ^a	NB ^a	Pt ^a	pH ^b	H ₂ ^c
1	+	-	+	-	6.1	42
1A	+	-	+	+	6.1	0
2	+	+	-	-	6.1	31
2A	+	+	-	+	6.1	0
3	+	-	+	-	4.0	96
3A	+	-	+	+	4.0	0
4	+	+	-	-	4.0	48
4A	+	+	-	+	4.0	0
5 ^d	-	-	-	-	4.0	387
5A ^d	-	-	-	+	4.0	176

^aThe concentrations used are as follows: 2-propanol, 0.2 M; acetone, 0.2 M; NB, 2 × 10⁻⁴ M; Pt, 4 × 10⁻⁴ M batch 0905. When a component is present a + sign is indicated, otherwise -. ^bBuffers were 0.0036 M acetate buffer⁷ for pH 4.0, 0.0040 M phosphate buffer⁷ for pH 6.1. ^cH₂ measured by GC, arbitrary units. ^dIn these experiments, 0.20 mL of H₂ was injected into 5 cm³ of gaseous phase equilibrated with solutions containing only the above 15 cm³ of buffer with Ptc added.

several differences. In the MV²⁺-Ptc system an equilibrium between MV⁺, MV²⁺, loaded Ptc, H⁺, and H₂ is established.^{6h} Above pH 7, significant amounts of MV⁺ exist in the equilibrium mixture. Moreover, at pHs above 10, the MV⁺ concentration at equilibrium exceeds the initial [MV⁺] produced by the pulse due to additional, Ptc-catalyzed, reduction of MV²⁺ ions by the molecular H₂ (produced in processes 1 and 2. Comparison of the redox potentials of NB/NB⁻ (-0.486)³ and MV²⁺/MV⁺ (-0.446)⁵ suggests that if similar processes take place in the two systems, the same effects will be observed in the Ptc/NB system, shifted by +1.3 pH units as compared to the Ptc-MV²⁺ system. This is because the redox potential of Ptc changes by 0.03 V with every pH unit as can be seen from 10.^{6h} However, in contrast to the

$$E(\text{Ptc}) = E^{\circ}(\text{Ptc}) - \frac{RT}{2F} \ln 1/[\text{H}^+] \quad (10a)$$

$$E(\text{Ptc}) = -0.082 - 0.03\text{pH} \quad (10b)$$

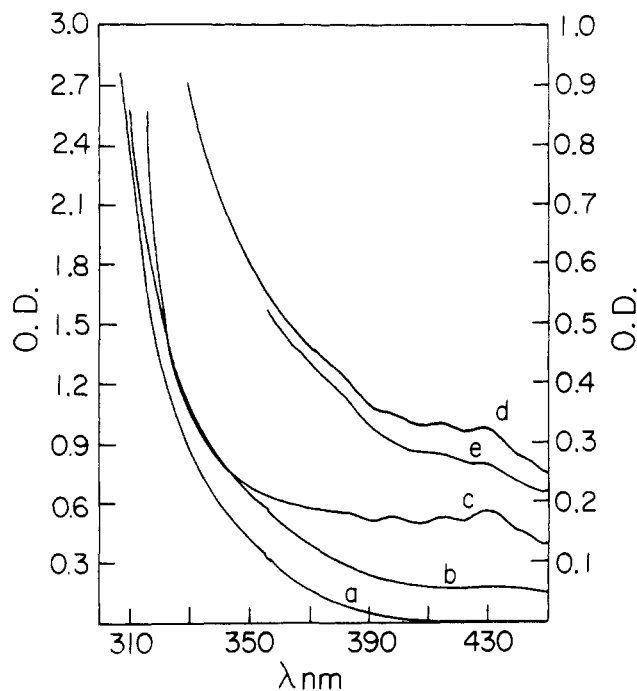


Figure 6. Effect of H₂ bubbling: (a) spectrum of 2 × 10⁻³ M NB at pH 12; (b) spectrum of 2 × 10⁻³ M NB + 4 × 10⁻⁵ M Ptc at pH 12; (c) spectrum of b immediately after H₂ bubbling; (d) spectrum of b 2 min later; (e) spectrum as in d after 5 min. (1) For (a) to (c), use the left-hand scale; for (d) and (e), use the right-hand scale. (2) Peaks are seen at 398, 414, and 430 nm and shoulders at 370, 380, and 442 nm.

Ptc-MV²⁺ system, the NB⁻ decays away to zero over the entire pH range investigated.

As expected, by analogy with the Ptc-MV²⁺ system, at pHs > 11.4 additional NB⁻ is produced through the reduction of NB by H₂ and equilibrium is first established between loaded Ptc, NB, H₂, H⁺, and NB⁻. This is followed by a complete decay of the NB⁻. At the lower pHs, no equilibrium is observed for NB⁻ and only the decay process is observed. In addition, several differences are observed in the kinetics. NB⁻ reacts with Ptc much slower than MV⁺. The rate constant is pH dependent and first order with respect to [Ptc], while no such pH dependence is observed in the MV²⁺ system^{6h} and an order higher than one with respect

(13) W. H. Smith and A. J. Bard, *J. Am. Chem. Soc.*, **97**, 5203 (1975), and references cited therein.

TABLE IV: Comparison of Observed and Theoretical Rate Constants of the Decay of NB⁻

pH	K_{ab}^a	f_{ab}^e	k_{ab}^c	k_{expt}^d	k_d^e
6.00	6080	0.39	9.7×10^7	9.7	20 ± 1
7.00	1890	0.49	6.1×10^7	6.1	
8.00	590	0.60	3.8×10^7	3.8	5.5 ± 2
8.20	476	0.62	3.4×10^7	3.4	3.5 ± 0.2
8.70	265	0.68	2.7×10^7	2.7	4.0 ± 0.5
9.00	183	0.73	2.3×10^7	2.3	1.8 ± 1
9.60	92.5	0.77	1.7×10^7	1.7	2.1 ± 0.5
9.80	73.2	0.79	1.5×10^7	1.5	0.6 ± 0.1
10.00	57.0	0.82	1.4×10^7	1.4	1.5 ± 0.3
10.75	24.1	0.88	9.2×10^6	0.9	0.55 ± 0.05
11.00	17.8	0.90	8.0×10^6	0.8	2.0 ± 0.2
11.40	11.2	0.93	6.5×10^6	0.6	0.3
12.00	5.5	0.96	4.6×10^6	0.5	0.2

^a K_{ab} is calculated as $10^{0.06(\Delta E^\circ)}$ by using the value of $E^\circ(\text{NB}^-/\text{NB}) = 0.486^3$ and E°_{Pt} according to eq 10. ^b Determined from eq 12. ^c Calculated from eq 11. ^d Expected first-order rate constant calculated $k_{ab}[\text{Ptc}]$, where the Ptc concentration is estimated to be 10^{-7} M. Since the formal concentration of Pt is 4×10^{-4} M and the value of 4000 is the estimated correction factor (see Experimental Section). ^e The values of k_d are averages taken from Table I.

to [Ptc] is obtained.⁶ Moreover, varying the NB concentrations had no effect on the rate of NB⁻ decay, again in contrast with the decay of MV⁺ where increasing the MV²⁺ decreased both the rate and the fraction of MV⁺ which decayed away.^{6h}

The differences between the MV²⁺-Ptc and the NB-Ptc systems are due to several reasons:

(a) NB⁻, unlike MV⁺, can be further reduced under our conditions. Stable two-, and four-, and six-electron reduction products of NB are known:¹⁰⁻¹⁶ nitrosobenzene (NOB), phenylhydroxylamine (PHA), and aniline. Under our conditions, PHA is expected to be the predominant final product. This conclusion is based on the redox potentials of the species involved. Polarographic measurements¹⁶ show that PHA is more easily produced, upon reduction of NB, as compared with NOB. On the other hand, further reduction to aniline is not feasible because of its too negative redox potential.¹⁶ In contrast to NB⁻ the redox potential of the loaded Ptc under our conditions is not sufficiently negative to reduce MV⁺ to MV⁰. This means that MV⁺ is only capable of loading Ptc while NB⁻ can also unload Ptc. Consequently, NB⁻ decays to zero concentration by a Ptc-catalyzed disproportionation to form NB and PHA, while MV⁺ remains as such in equilibrium with loaded Ptc. This also explains the yellow color of the intermediate observed in the H₂ bubbling experiments (Figure 6). We suggest that the spectrum is of the recently reported NOB⁻¹⁵ since neither NB⁻^{10,11} (which is ruled out also for lifetime reasons), nor NOB¹⁷ or PHA¹⁸ possess an absorbance in that region.

(b) NB⁻ reacted with Ptc much slower than did MV⁺. This may be due to, at least in part, the negative charge which the Ptc possesses even before any loading took place.^{6h} The negative charge of the colloidal particles repelled the NB⁻ but attracted the MV⁺; therefore the difference in rates of reaction in these two systems is not surprising.

(c) In the NB-Ptc system we found that the decay rate of NB⁻ is proportional to $[\text{H}^+]$ to the power of 0.5 ± 0.1 . No similar dependence was observed in the MV²⁺-Ptc system.^{6h} As mentioned above, NB⁻ reacts with Ptc relatively slowly, far below the diffusion-controlled rate. The Marcus theory¹⁹ predicts that the rate of an electron-transfer reaction will vary with the redox

potential of the system involved according to

$$k_{ab} = (k_{aa}k_{bb}K_{ab}f_{ab})^{1/2} \quad (11)$$

where f_{ab} is defined by

$$\log f_{ab} = \frac{(\log K_{ab})^2}{4 \log (k_{aa}k_{bb}/Z^2)} \quad (12)$$

K_{ab} is the equilibrium constant for the redox system and is related to its redox potential. The values of k_{aa} and k_{bb} are the exchange rate constants for each of the reacting redox systems, respectively. They were taken as $2 \times 10^5 \text{ M}^{-1} \text{ s}^{-1}$ for NB⁻/NB,²⁰ and assumed to be $2 \times 10^7 \text{ M}^{-1} \text{ s}^{-1}$ for the Ptc system. Z is the collision frequency, taken here as 10^{11} . On the basis of eq 10²¹ and 11, the rate constant for the loading reaction of Ptc by NB⁻, k_{ab} , can be shown to depend linearly on $[\text{H}^+]^{1/2}$, in agreement with the experimental data. Table IV presents a comparison between the experimental and calculated values of k_{ab} . This dependency on $[\text{H}^+]^{1/2}$ is not observed in the MV²⁺-Ptc system, probably because in that case the reaction of MV⁺ with "naked" Ptc is diffusion controlled.

(d) Another difference between NB-Ptc and MV²⁺-Ptc is the order of the decay of the reduced species with respect to the [Ptc]. In acid solutions the decay of MV⁺ is second order in [Ptc]. The order is >1 at near neutral pHs. This has been previously explained by assuming that only "naked" colloidal particles were active^{6h} toward the MV⁺. This means that the stabilizer was assumed to prevent the MV⁺ from reaching the Ptc. The "naked" colloid was suggested to be formed as a result of a two-particle collision, leading to second-order dependence of the MV⁺ decay on Ptc at the acidic pHs when loading is the rate-determining step. In the near-neutral and basic solutions, the order in Ptc was less than 2 because of a significant contribution of the back-reaction which is first order in Ptc.^{6h} We suggest that the first-order dependence on Ptc at all pHs studied when NB⁻ reacts is due to the smaller size of NB⁻ as compared with MV⁺. This enables the NB⁻ to penetrate through the stabilizer molecules and reach the Ptc, so no bimolecular collision of the colloids is required.

Conclusions

NB⁻ (as well as MV⁺) can be obtained photochemically by electron transfer from an appropriate photosensitizer to NB. As in the case of MV⁺, it possesses a sufficiently negative redox potential to enable the reduction of water to hydrogen. Both MV⁺ and NB⁻ are able to load the Pt colloidal particles with reducing equivalents (in the form of hydride^{6h}). In the MV⁺ case, further reduction of the viologen is not possible under our conditions and hence only water can be reduced. In the NB⁻ case, no water is reduced because of the reduction of NB⁻ to phenylhydroxylamine. From the thermodynamical point of view, there is not much difference between these two processes, as far as photochemical energy storage is concerned. The NB system seems to be irre-

(20) D. Meyerstein, J. Rabani, M. S. Matheson, and D. Meisel, *J. Phys. Chem.*, **82**, 1879 (1978).

(21) We are aware that the Marcus theory can be applied to an elementary process only. Our phenomenological treatment still calls for a rigorous analysis based on a detailed mechanism of the loading process.

The Marcus theory is invoked in order to suggest that the $[\text{H}^+]^{1/2}$ dependency, although not a priori anticipated, does not disagree with the observations made in the various Ptc-reductant systems. For example, we may assume that the loading process involves a relatively slow electron transfer step from NB⁻ to the platinum colloid particle, which is loaded with a 2:1 electrons to protons ratio,^{6h} PtcH_nⁿ⁺, followed by fast protonation and additional electron transfer from another NB⁻ radical ion. An $[\text{H}^+]^{1/2}$ dependence of the loading rate constant can be calculated by using eq 10 and

$$K = A'e^{-\Delta G^*/RT} \quad (14)$$

if in addition we assume that $\Delta G^* = \Delta G$, namely, that practically no activation barrier exists for the back-reaction of NB with PtcH_n⁽ⁿ⁺¹⁾⁺. (A' is the collision frequency, ΔG^* is the free energy of activation).

An alternative way to rationalize the $[\text{H}^+]^{1/2}$ dependency is to consider the Pt colloidal particles as microelectrodes and assume that the protonation of the loaded Ptc is the predominant factor determining the metal-solution potential difference. (R. A. Marcus, private communication.)

(14) G. Pezzatini, and R. Guidelli, *J. Electroanal. Chem.*, **102**, 205 (1979).

(15) C. Nishihara and M. Kaise, *J. Electroanal. Chem.*, **149**, 287 (1983), and references cited therein.

(16) I. M. Kolthoff and J. J. Lingane, "Polarography", Vol. II, 4th ed, Interscience, New York, 1965, p 7489.

(17) "Beilstein Handbuch der Organischer Chemie", Vol. E. IV 5, p 703 (system no. 465).

(18) Reference 17, Vol. E III 15, p 5 (system no. 1932).

(19) R. A. Marcus, *Discuss. Faraday Soc.*, **29**, 21 (1960); *J. Phys. Chem.*, **67**, 853 (1963).

versibly reduced. This may have an advantage if energy storage is concerned because it prevents the back oxidation reaction by oxygen, if simultaneously generated in the same reacting cell. Hydrogen quickly loads the Ptc particles and its reaction with O₂ is expected to be efficiently catalyzed by Ptc, while the four-electron NB reduction product, PHA, once produced, may be stable in the presence of both Ptc and O₂.

Acknowledgment. The authors are indebted to M. Brandeis, A. Henglein, and R. A. Marcus for helpful discussions. This research was supported by the Israeli NCRD and by the Balfour and Schreiber Foundations.

Registry No. NB, 98-95-3; NB⁻, 12169-65-2; PHA, 100-65-2; NOB, 586-96-9; H₂, 1333-74-0; Pt, 7440-06-4; 2-propanol, 67-63-0.

Effect of Pressure on the Raman Spectra of Solids. 2. Pyridine

A. M. Heyns* and M. W. Venter

Department of Chemistry, University of Pretoria, 0002 Pretoria, South Africa (Received: January 22, 1985; In Final Form: May 8, 1985)

Two modifications of pyridine have been identified when the liquid is solidified at 10 kbar in a diamond anvil cell at 300 K. The effect of pressure on the Raman spectra of these modifications is reported. The one modification is crystalline and characterized by narrow and well-defined lattice modes and undergoes a phase transition at 20 kbar, while the other has fewer and much broader lattice vibrations. The Raman spectra of none of these modifications are in agreement with the space group reported for solid pyridine obtained by cooling the liquid at atmospheric pressures. The pressure dependence of the Raman bands of the crystalline phase indicates that it possibly corresponds to the monoclinic phase II in planar, aromatic molecules such as benzene, while the other modification possibly resembles the glassy phase observed in infrared experiments. The internal modes of solid pyridine in all the phases closely resemble those of the liquid.

Introduction

Numerous experimental and theoretical studies on the vibrational spectra of pyridine and deuterated pyridines have appeared in the literature.¹⁻¹⁷ These studies dealt mainly with the liquid and vapor phases of pyridine, although some studies on the vibrational spectra of the solid phase were published.^{8,18} Two crystalline modifications of pyridine have been characterized by X-ray methods.¹⁹ These modifications (D_{2h}^1 and D_{2h}^2) do not show great differences and the conditions for the conversion of the one into the other were not established. A glassy state of pyridine was obtained when the vapor was deposited onto a cold CsI window; it changed to a crystalline state upon warming and in solid pyridine-*d*₅ a phase transition was observed that could not be detected in pyridine itself.⁸ A subsequent crystal structure analysis of single crystals of pyridine revealed that it has an unexpectedly complicated crystal structure with 16 molecules per unit cell.²⁰ Compared to the polymorphism of solid benzene which has been carefully studied²¹⁻²³ very little is known about the

corresponding behavior of solid pyridine, particularly at high pressures.

Experimental Section

Details regarding the equipment used have already been published.²⁴ The hole in the Inconel gasket in the diamond anvil cell was loaded with a purified sample of pyridine and a ruby chip. The pyridine was purified by refluxing over KOH for at least 24 h and then fractionally distilled. The pressure conditions prevailing inside the cell were monitored according to the R₁ and R₂ lines of the ruby to determine whether there were hydrostatic conditions inside the cell. The spectral resolution of the bands reported is approximately 3 cm⁻¹.

Results

Upon compression of the liquid pyridine sample, solidification occurs at ~10 kbar in both pyridine and pyridine-*d*₅. The full spectra of the solid samples are summarized in Tables I and II; the lattice modes of pyridine are shown in Figure 1 and these results are summarized in Table III.

The Raman spectra of solid pyridine and pyridine-*d*₅ do not display a multiplicity of bands and closely resemble the corresponding ones in the liquid phase, excepting of course the occurrence of lattice modes and a general upward shift in most of the internal modes of the solid samples. In a very limited number of Raman bands in solid pyridine-*d*₅ either a splitting of bands occurred (e.g., ν_1 at 971 and 978 cm⁻¹ at 11 kbar) or asymmetries developed (e.g., ν_{12} at 1006 and 1015 cm⁻¹ at 11 kbar). The Raman spectrum of solid pyridine recorded at low temperatures at ambient pressures also did not show a multiplicity of bands,⁸ in direct contrast to the infrared spectra reported in the same study. Since relatively simple spectra of solid pyridine and pyridine-*d*₅ were obtained the assignment of the internal modes could be done

- (1) Turkevich, J.; Stevenson, P. C. *J. Chem. Phys.* **1943**, *11*, 328.
- (2) Kline, C. H.; Turkevich, J. *J. Chem. Phys.* **1944**, *12*, 300.
- (3) Corrsin, L.; Fax, B. J.; Lord, R. C. *J. Chem. Phys.* **1953**, *21*, 1170.
- (4) Wilmshurst, J. K.; Bernstein, H. J. *Can J. Chem.* **1957**, *35*, 1183.
- (5) Long, D. A.; Murfin, F. S.; Thomas, E. L. *Trans. Faraday Soc.* **1963**, *59*, 12.
- (6) Zerbi, G.; Crawford, Jr., B.; Overend, J. *J. Chem. Phys.* **1963**, *38*, 127.
- (7) Innes, K. K.; Byrne, J. P.; Ross, I. G. *J. Mol. Spectrosc.* **1967**, *22*, 125.
- (8) Castellucci, E.; Sbrana, G.; Verderame, F. D. *J. Chem. Phys.* **1969**, *51*, 3762.
- (9) Suzuki, S.; Orville-Thomas, W. J. *J. Mol. Struct.*, **1977**, *37*, 321.
- (10) Kakiuti, Y.; Akiyama, M.; Saito, N.; Saito, H. *J. Mol. Spectrosc.* **1976**, *61*, 164.
- (11) Mochizuki, Y.; Kaya, K.; Ito, M. *J. Chem. Phys.* **1978**, *69*, 935.
- (12) Harsányi, L.; Kilar, F. *J. Mol. Struct.* **1980**, *65*, 141.
- (13) Stidham, H. D.; DiLella, D. P. *J. Raman Spectrosc.* **1979**, *8*, 180.
- (14) DiLella, D. P.; Stidham, H. D. *J. Raman Spectrosc.* **1980**, *9*, 90.
- (15) DiLella, D. P. *J. Raman Spectrosc.* **1980**, *9*, 239.
- (16) Stidham, H. D.; DiLella, D. P. *J. Raman Spectrosc.* **1980**, *9*, 247.
- (17) Pongor, G.; Pulay, P.; Fogarasi, G.; Boggs, J. E. *J. Am. Chem. Soc.* **1984**, *106*, 2765.
- (18) Loisel, J.; Lorenzelli, V. *J. Mol. Struct.* **1967**, *1*, 157.
- (19) Biswas, S. G. *Indian J. Phys.* **1958**, *32*, 13.
- (20) Mootz, D.; Wussow, H. G. *J. Chem. Phys.* **1981**, *75*, 1517.

- (21) Akella, J.; Kennedy, G. C. *J. Chem. Phys.* **1971**, *55*, 793.
- (22) Ellenson, W. D.; Nicol, M. *J. Chem. Phys.* **1974**, *61*, 1380.
- (23) Adams, D. M.; Appleby, R. *J. Chem. Soc., Faraday Trans. 2*, **1977**, *73*, 1896.
- (24) Heyns, A. M.; Clark, J. B. *J. Raman Spectrosc.* **1983**, *14*, 342.